Plume model for the boundary-layer dynamics in hard turbulence

J. Werne
Advanced Study Program, National Center for Atmospheric Research, Boulder, Colorado 80307
(Received 28 January 1994)

"Hard turbulence" has come to be associated with several features of high-Rayleigh-number Boussinesq convection: thermal plumes, intermittency, nonclassical Nu-Ra scaling ($\mathrm{Nu} \propto \mathrm{Ra}^{2/7}$), large-scale circulation, and the strongly sheared thermal boundary layers that result. In this paper, we make use of one of these features, the plumes, to offer an explanation of recent measurements of "waves" propagating on the boundary layers. The measured "dispersion relation" is reproduced here by a scaling theory incorporating the drag force of buoyant plumes and the interaction of these plumes with the boundary layers.

PACS number(s): 47.27.Ak, 47.27.Cn

In recent years, high-Rayleigh-number Boussinesq convection [1] has received much attention as a model problem for transitions to turbulence [2]. The problem is a classic one of a fluid heated from below wherein the nondimensional Rayleigh number $\mathrm{Ra}=\alpha g \Delta L^3/(\nu\kappa)$, is a control parameter measuring the strength of the temperature difference Δ driving the flow: g is the acceleration due to gravity; L is the height of the fluid layer; and α, ν, and κ are the fluid's thermal expansion coefficient, kinematic viscosity, and thermal diffusivity, respectively. The experiments of Libchaber and his collaborators have been instrumental in outlining the nature of the transitions to turbulence as Ra is increased and have defined the "nonclassical" regime of hard turbulence for $\mathrm{Ra} > \mathrm{Ra}_T$ [$\approx 4\times 10^7$ for a unit aspect (width-to-height) ratio container]. At the time this new state was discovered, thermal plumes were hypothesized to be one of its defining features [2]. Later, visualizations in water at $\mathrm{Ra} \approx \mathrm{Ra}_T$ verified that coherent structures (i.e., plumes) do indeed appear at the onset of hard turbulence [3], developing out of an instability of the thin, diffusive, thermal boundary layers attached to the heated and cooled bottom and top surfaces of the cell [4].

The existence of thermal plumes as they appear in hard turbulence can be understood simply as the nonlinear development of the Rayleigh-Taylor instability [5] at the thin thermal boundary layers. However, the plumes' formation and subsequent effect on the mean flow are coupled to the strong shear maintained at the boundaries by the large-scale circulation existing in hard turbulence [6]. An outstanding question has been, "What governs the formation of these thermal plumes." Attempts to answer this question have concentrated on characterizing the early stage of plume formation as a wave [3,7].

The inception of this wave theory has been motivated primarily by the highly suggestive images produced by Zocchi, Moses, and Libchaber [3] using water in a unit aspect ratio cell and liquid crystal pellets that change color in accord with the water's temperature [3]. In this way, Zocchi, Moses, and Libchaber have observed wavelike patterns on a boundary layer in hard turbulence (see plate I of Ref. [3]). They go on to measure the "dispersion relation" for these "waves" and suggest a fit to their data of $v_l \propto l^{1/2}$, where v_l is the velocity of a "wave" of size l. Though this expression only captures the qualitative trend in the experimental data and does not fit its detailed structure (see Fig. 6 of Ref. [3]), Zocchi, Moses, and Libchaber are encouraged that its form is identical to a well-known wave-dispersion relation—that of gravity waves; they are quick to point out, however, that an identification of the "waves" they observe as gravity waves is less than satisfying given that the boundary layers are unstably stratified and therefore posses no gravitational restoring force for wave motion. A final complication for any wave-based theory, which Zocchi, Moses, and Libchaber appreciate and point out, is that their collection of measurements exhibits an unusually larger scatter to be attributable to a wavelike dispersion relation; indeed, Zocchi, Moses, and Libchaber must average all values of v_l obtained for a given l before a "dispersion relation" is discernible.

An alternate interpretation of the "waves" visualized by Zocchi, Moses, and Libchaber is provided by Shelley and Vinson [7] who construct a simple two-dimensional (2-D) model of a sheared thermal boundary layer in an attempt to understand the formation, morphology, and motion of plumes. Neutrally stable traveling waves exist for this model and, as Shelley and Vinson have pointed out, the dispersion relation does not agree, even in a qualitative sense, with the experimental results of Zocchi, Moses, and Libchaber: The model predicts slow propagation of waves possessing the longest wavelengths and propagation of the smallest-wavelength waves with the free-stream velocity just outside the thermal boundary layer. The experiment of Zocchi, Moses, and Libchaber, on the other hand, demonstrates just the opposite: Small-wavelength disturbances on the thermal boundary layer are correlated with low velocities, while the largest-wavelength disturbances move *faster* than the mean free-stream velocity. Shelley and Vinson explain this discrepancy by suggesting that "... the observed waves reflect some other collective action of the system." Recent numerical simulations of 2D hard turbulence reported by Werne support this interpretation [8].

Figure 1 presents a sequence of images of the cold thermal boundary layer from the 2D numerical simulations in Ref. [8]. A careful study of the Figure illuminates the mechanism giving rise to plume formation in the simulations. Furthermore, this mechanism suggests a simple model which correctly predicts the structure of the velocity–length-scale correlations (i.e., the "dispersion relation") measured by Zocchi, Moses, and Libchaber. The first image in the sequence [Fig. 1(a)] shows the impact of the cold boundary layer by a large hot plume which has been ejected from the opposite boundary. This hot plume has traveled with the large-scale circulation up along the left sidewall. Once it reaches the upper left corner in the cell and impacts the leftmost edge of the cold boundary layer, it is redirected horizontally along the upper boundary layer. As it moves to the right along the cold boundary layer [Figs. 1(b)–1(d)], it drags a good deal of cold fluid with it. In this way, a small cold "plume" (i.e., a disturbance on the cold thermal boundary layer) is born and driven across the cell. By the time the newly formed cold "plume" is forced to the right side of the cell [Fig. 1(d)], its horizontal velocity is reduced by the increasing adverse pressure gradient which exists as a result of the right sidewall. At the right side of the cell, several (≈ 2 to 4 for simulations with $\mathrm{Ra}=8.192\times10^7$) of these small "plumes" coalesce to form a single large plume; this coalescence is evident in Figs. 1(a)–1(e). The dynamics of the large plume which results is eventually dominated by gravity, causing the plume to plunge towards the lower boundary [Figs. 1(f)–1(h)] where it continues the process.

Note that this picture of plume formation does not incorporate waves on the boundary layer. Though few plumes may develop from the nonlinear growth of traveling waves during quiescent periods, most of the plumes in the simulations are initiated by the bombardment of large plumes ejected from the opposite boundary layer. (This may also have been the case for the experiments of Zocchi, Moses, and Libchaber; however, we cannot know because the liquid crystal used for the visualizations had a color response of only $\Delta/2$ or less and therefore could not simultaneously indicate the temperature of a boundary layer and the large plumes emitted from the opposite boundary.) Because the boundary layer's bombardment by plumes is continual, it is questionable that a dispersion relation characteristic of traveling waves would be evident at all. It is more likely that the velocity–length-scale correlations observed by Zocchi, Moses, and Libchaber tell us about the characteristics of the bombarding plumes themselves rather than about the oscillatory modes of the boundary layer which they impact. With this motivation, we attempt to understand the observed "dispersion relation" by first considering the forces acting on large plumes *before* they impact the boundary lay-

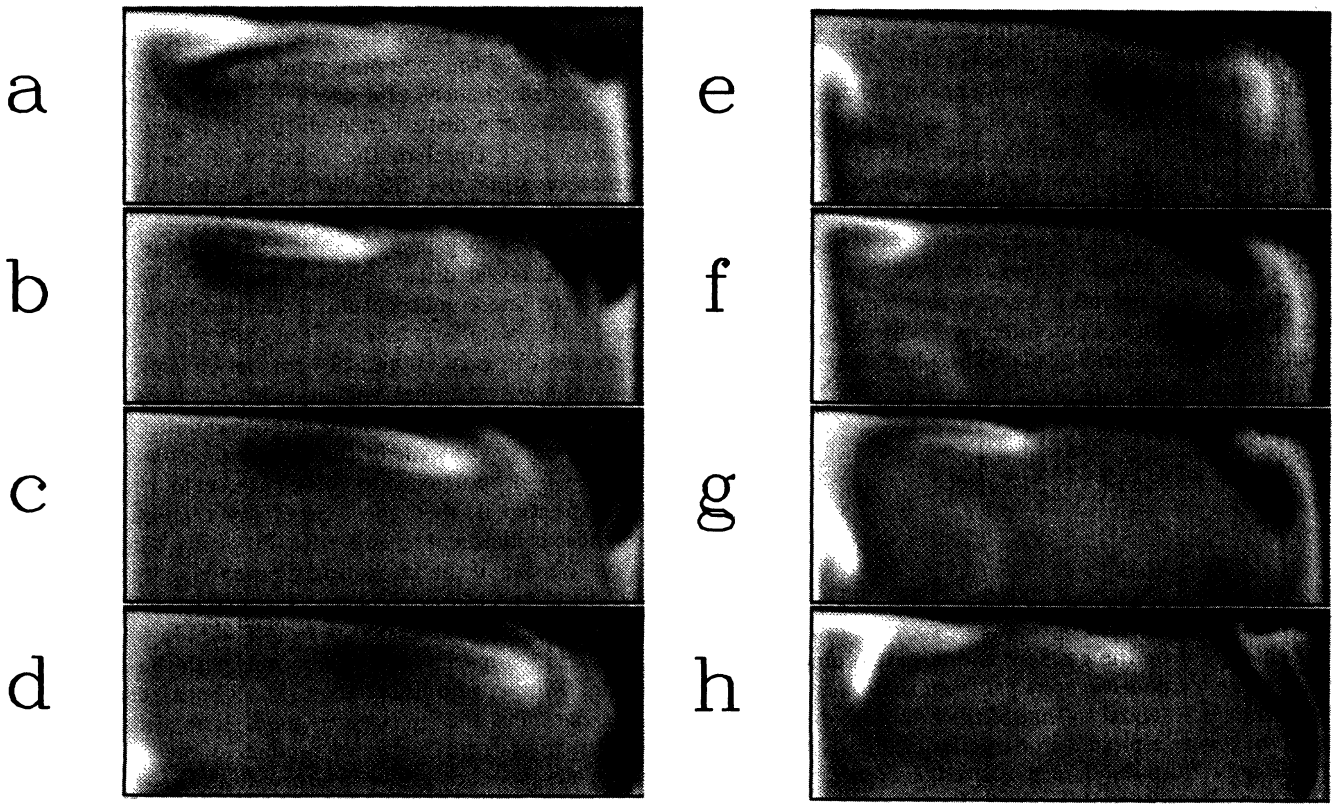

FIG. 1. Formation of a cold plume on the top thermal boundary layer with $\mathrm{Ra}=8.192\times10^7$ and $\sigma=7$ (from the numerical results of Werne [8]). White (black) represents hot (cold) fluid. Each image shows the top 38% of the cell. Time advances by $1.5\times10^{-4}L^2/(4\kappa)$ between each image, with a being the earliest in the sequence. (a)–(d) depict the development of cold "disturbances" as a hot plume impacts the upper boundary layer. Several of these disturbances coalesce (a)–(b) to form a cold plume which detaches near the right corner (f)–(h).

er. For a large hot plume, free of either boundary layer, the primary forces acting are the buoyancy force $F_B=\rho_0 Vg$; the gravitational force $F_g=-\rho Vg$; and the drag force $F_D=-C_D S\rho_0 v^2/2$, where V is the volume of fluid encompassed by the plume, C_D is the plume's drag coefficient, and S is the surface area of the plume on which the drag force acts. ρ and ρ_0 are the densities of the plume and the ambient fluid, respectively. The equation of motion of the plume then becomes

$$\frac{dv}{dt}=\frac{1}{2\Lambda}(c^2-v^2) ,$$

where

$$c^2=\left[\frac{\rho_0-\rho}{\rho_0}\right]\left[\frac{V}{S}\right]\left[\frac{2g}{C_D}\right] , \tag{1}$$

$$\Lambda=\left[\frac{\rho}{\rho_0}\right]\left[\frac{V}{S}\right]\left[\frac{1}{C_D}\right] .$$

Here, c is the terminal velocity of the plume and Λ is a characteristic length scale for plume acceleration. The drag coefficient C_D has the general form $C_D=C_1\mathrm{Re}^{-\gamma}$, where C_1 is a constant and Re is the Reynolds number of a plume, $\mathrm{Re}=vl/\nu$. The exponent γ depends on both the plume's shape and its orientation to the mean flow [9]. Though hard turbulence produces plumes of varying shapes, on the average plumes are much longer than they are thick ($l\gg\lambda$, where $l=$ plume length and $\lambda=$ plume thickness) and are aligned parallel to the mean flow when they travel vertically along the cell's sidewalls. Furthermore, for the experiment of Zocchi, Moses, and Libchaber, the flow around individual plumes is laminar, i.e., not turbulent: For $\mathrm{Ra}=1.1\times10^9$, the maximum Re obtained by the largest plumes is $\mathrm{Re}\approx(6\text{ mm/s})(180\text{ mm})/(1\text{ mm}^2/\text{s})\approx10^3$, (Ref. [10], while the transition to turbulence occurs at $\mathrm{Re}\approx10^6$ for objects with this shape. Hence, we should use $\gamma=\frac{1}{2}$, appropriate for thin objects aligned with a laminar flow, i.e., objects whose drag is dominated by "skin friction" as opposed to "pressure drag" [11]. The plume's terminal velocity then becomes

$$c=\left[\left[\frac{\rho_0-\rho}{\rho_0}\right]\lambda\left[\frac{2g}{C_1}\right]\left[\frac{l}{\nu}\right]^{\gamma}\right]^{1/(2-\gamma)} \tag{2}$$

or

$$c_l\propto l^{1/3}\quad\text{for }\gamma=\tfrac{1}{2} . \tag{3}$$

Note that Eq. (3) is true only if $(\rho_0-\rho)/\rho_0$ is independent of l, which will be the case for the largest plumes whose temperature (or density) contrast from their surroundings will be maximal (equal to that of the boundary layer from which they were ejected). For smaller plumes which were formed only from fluid near the edge of the boundary layer, the density contrast will be somewhat smaller. If we assume that the size of a plume, l, is indicative of the greatest depth into the boundary layer d which participated in the plume's formation, i.e., $d\propto l$, then we have from $(\rho_0-\rho)/\rho_0\propto d$ that $(\rho_0-\rho)/\rho_0\propto l$. [$(\rho_0-\rho)/\rho_0\propto d$ is obtained by noting that the temperature profile within a boundary layer is approximately linear.] Therefore, for these smaller plumes, for which d is less than the boundary-layer thickness, Eq. (2) becomes

$$c_l\propto l^{(1+\gamma)/(2-\gamma)} \tag{2'}$$

or

$$c_l\propto l\quad\text{for }\gamma=\tfrac{1}{2} . \tag{3'}$$

These terminal velocities [Eqs. (3) and (3')] will be attained by plumes (large and small, respectively) if $L-(\delta t)U\gg\Lambda$, where δt is the time required for the plume to move between the bottom and top boundaries and U is the speed for the background roll. This constraint is equivalent to

$$\frac{U+v}{v}\ll\frac{L}{\Lambda} , \tag{4}$$

where v is the plume's velocity *relative to the roll.* With the recent measurements by Tilgner, Belmonte, and Libchaber, we estimate $U<5.5$ mm/s and $v>1.7$ mm/s, and hence $(U+v)/v\approx4$, for $\mathrm{Ra}=1.1\times10^9$ [10]. In addition, $\Lambda\approx\lambda$ since both C_D and ρ/ρ_0 are ≈1 [see Eq. (1)]. Furthermore, because λ is roughly the thermal boundary-layer thickness, $L/\Lambda\approx2\mathrm{Nu}\approx260$ at the same values of Ra [12]. Therefore, Eq. (4) is clearly satisfied, and plumes will reach their terminal velocity in traveling between the boundaries.

In order to correlate velocities and length scales of disturbances on the boundary layer, we must evaluate the effectiveness of the incoming plumes, described above, to produce disturbances of a given size and velocity. First, the velocity of a disturbance on the boundary layer v_{bl} is approximately equal to the velocity of the bombarding plumes creating the disturbance, $v_{\mathrm{bl}}\approx c_l$: As the large plume travels along the boundary layer, it drags fluid from the boundary layer with it. Second, larger plumes give rise to larger disturbances: The larger the impacting plume, the more momentum it can exchange with the fluid in the boundary layer. Thus, like the relationships represented in Eqs. (3) and (3') for buoyant plumes moving with their terminal velocity, larger disturbances on the boundary layer move with larger velocities. Furthermore, if the length scale of the disturbance on the boundary layer is proportional to the length scale of the plume which created it, then the "dispersion relation" for disturbances is identical to either Eq. (3) or Eq. (3'), depending on the size of the impacting plume. Hence, for small, slow disturbances, we expect $v_l\propto l$, while for large, fast disturbances, we should observe $v_l\propto l^{1/3}$ [13].

Figure 2 compares these predictions with the data from Zocchi, Moses, and Libchaber [3]. The agreement between data and theory is quite good. The abruptness of the transition from the $v_l\propto l$ regime to the $v_l\propto l^{1/3}$ regime lends credence to our interpretation that this transition results when plumes become large enough to obtain the maximum possible density contrast characteristic of the boundary layers. Furthermore, the velocity at the transition point, v_t, provides a valuable consistency check for the present theory. Computing the terminal velocity from Eq. (1) [estimating λ and C_D as before and comput-

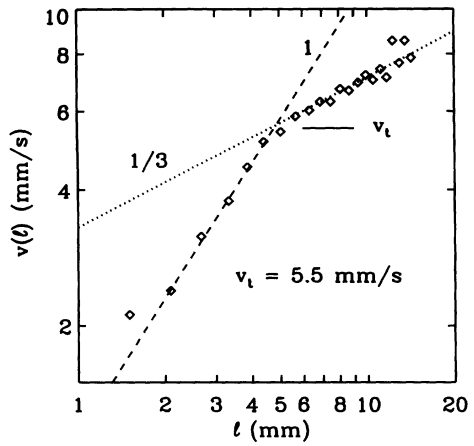

FIG. 2. Velocity–length-scale correlations for disturbances on the thermal boundary layers in hard turbulence. The experimental data of Zocchi, Moses, and Libchaber [3] is presented along with the power laws (arbitrary normalization) predicted by the present theory.

ing $(\rho_0-\rho)/\rho_0=\alpha\Delta/2$ with $\Delta=8\,^{\circ}\mathrm{C}$, as in Zocchi, Moses, and Libchaber], we obtain $c_t\approx 5.1$ mm/s, in excellent agreement with the experimental value of $v_t=5.5$ mm/s.

A noteworthy consequence of this simple picture of plume formation is a simple explanation of the possibility of disturbances moving *faster* than the mean free-stream velocity just outside the thermal boundary layer. Indeed, the largest plumes contribute a substantial positive fluctuation to the mean "wind." Disturbances created by these largest plumes must, therefore, move faster than the mean wind.

It should also be pointed out that this simple picture easily explains the large scatter in the raw data of Zocchi, Moses, and Libchaber: Bombarding plumes with different shapes necessarily have different drag coefficients C_D and, hence, different terminal velocities; therefore, different plumes which give rise to disturbances on the boundary layer with the same length scale, l_{bl}, may strike the boundary layer with a large range of velocities. It is only when the average plume of a given size l is considered that the velocity–length-scale correlation becomes apparent.

An important point should be made concerning the robust nature of the prediction that large disturbances on the boundary layers move faster than small ones. In particular, the detailed properties of plumes [specifically, $\gamma=\frac{1}{2}$ and $(\rho_0-\rho)/\rho_0\propto l$ for small plumes but is independent of l for large plumes] are unnecessary to conclude that large disturbances *must* move faster than small ones within the general framework of this simple theory. To illustrate, if we consider general γ and $(\rho_0-\rho)/\rho_0\propto l^{\beta}$, we obtain $v_l\propto l^{(\beta+\gamma)/(2-\gamma)}$, the exponent of which will be positive if $\beta+\gamma>0$ (since γ takes on a maximum value of 1 for "creeping flow" [9], restricting $2-\gamma>0$). Furthermore, note that β must be positive because larger plumes, produced as a result of more violent eruptions of the thermal boundary layers, are more intense than smaller plumes. Also, γ will be positive unless the plume moves so quickly with respect to the surrounding fluid that it develops a turbulent boundary layer on its own "surface" (and experiences the "drag crisis") [9]. This will not occur for $\mathrm{Ra}=1.1\times 10^9$ because the plumes are "laminar." It follows quite generally, therefore, that v_l must scale with a positive power of l. It would be interesting to discover if the velocity–length-scale correlations exhibit a qualitative difference when Ra is higher and the plumes become turbulent.

CONCLUSION

In summary, the experimental velocity–length-scale correlation for disturbances propagating on the boundary layers in hard turbulence is reproduced here by a simple scaling theory. The crucial step in the analysis is to abandon the notion that the observed disturbances are waves propagating along the boundary layers and to recognize that these disturbances result from plumes bombarding the boundary layers. Properties of the plumes, primarily the drag they experience and their density contrast, are used to construct the theory; the measurement of these properties would prove useful in evaluating the validity of specific assumptions made in the theory. Nevertheless, a general prediction of this theory is that large disturbances on the boundary layers move faster than small ones, regardless of specific assumptions concerning the detail properties of plumes.

ACKNOWLEDGMENTS

I would like to thank Giovanni Zocchi for permitting the use of his experimental data. In addition, I would like to acknowledge illuminating conversations with Mike Leibig, Bob Rosner, Mike Shelley, and Peter Sullivan and extend thanks to Fausto Cattaneo and Ed DeLuca for producing the numerical algorithm whose solutions have offered so much insight into the working of hard turbulence over the past few years. NCAR is sponsored by the National Science Foundation.

[1] S. Chandrasekhar, *Hydrodynamic and Hydromagnetic Stability* (Oxford University Press, New York, 1961).

[2] F. Heslot, B. Castaing, and A. Libchaber, Phys. Rev. A **36**, 5870 (1987).

[3] G. Zocchi, E. Moses, and A. Libchaber, Physica A **166**, 387 (1990).

[4] Thin thermal boundary layers develop on the hot and cold surfaces of the cell as a result of heat diffusion: While the heat flux in the turbulent interior of the cell may be transported by fluid motion, the flux into and out of the cell must be carried totally by diffusion, given the no-slip (velocity equal to zero) condition at the cell boundaries.

[5] Lord Rayleigh, Philos. Mag. **32**, 529 (1916).

[6] M. Sano, X. Z. Wu, and A. Libchaber, Phys. Rev. A **40**,

6421 (1989).
[7] M. J. Shelley and M. Vinson, Nonlinearity **5**, 323 (1992).
[8] J. Werne, Phys. Rev. E **48**, 1020 (1993).
[9] See any introductory engineering text on fluid mechanics, e.g., F. M. White, *Fluid Mechanics* (McGraw-Hill, New York, 1979).
[10] A. Tilgner, A. Belmonte, and A. Libchaber, Phys. Rev. E **47**, R2253 (1993).
[11] The analysis of plume drag, resulting with $C_D = C_1 \mathrm{Re}^{-1/2}$, is identical to that for a laminar flat-plate boundary layer; see H. Schlichting, *Boundary-Layer Theory* (McGraw-Hill, New York, 1979). Geometrical differences between plumes and a flat plate alter the normalization coefficient C_1 but not the scaling exponent $\frac{1}{2}$.
[12] S. Gross, G. Zocchi, and A. Libchaber, C. R. Acad. Sci. **307**, 447 (1988).
[13] For low σ, one expects $v \propto l^{1/2}$ for small plumes and $v = \text{const}$ for large plumes given that thermal structures are much more diffuse for $\sigma \ll 1$ and will hence be dominated by "pressure drag" ($C_D = \text{const}$).

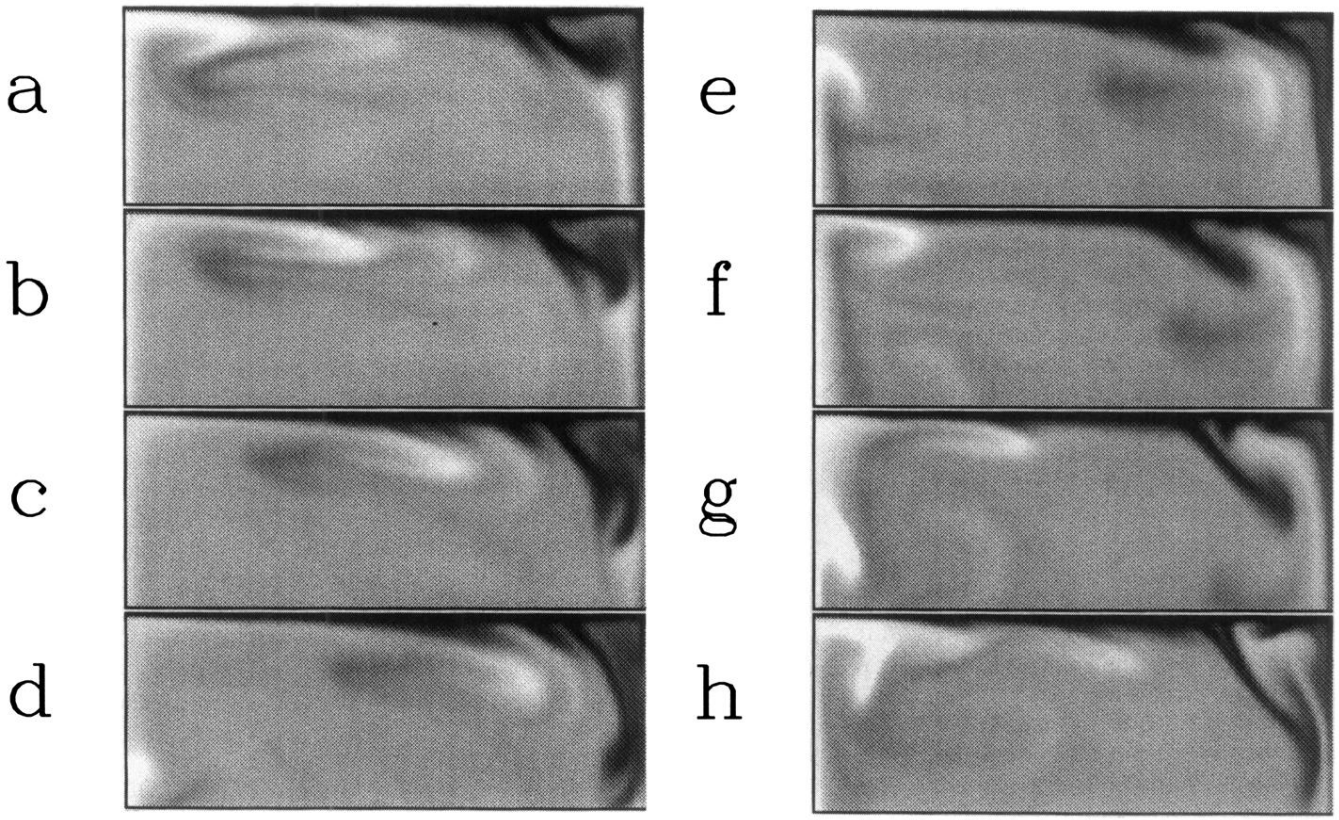

FIG. 1. Formation of a cold plume on the top thermal boundary layer with $\mathrm{Ra}=8.192\times10^{7}$ and $\sigma=7$ (from the numerical results of Werne [8]). White (black) represents hot (cold) fluid. Each image shows the top 38% of the cell. Time advances by $1.5\times10^{-4}L^{2}/(4\kappa)$ between each image, with a being the earliest in the sequence. (a)–(d) depict the development of cold "disturbances" as a hot plume impacts the upper boundary layer. Several of these disturbances coalesce (a)–(b) to form a cold plume which detaches near the right corner (f)–(h).